Degradation of Solid Oxide Electrolyser Cells with Different Anodes

Cheng Xu, Yin Wang, Le Jin, Junfeng Ding, Xiao Ma and Wei Guo Wang

ECS Trans. 2012, Volume 41, Issue 33, Pages 97-102.
doi: 10.1149/1.3702416

ECS Transactions, 41 (33) 97-102 (2012)
10.1149/1.3702416 ©The Electrochemical Society

Degradation of Solid Oxide Electrolyzer Cells with Different Anodes

C. Xu, Y. Wang, L. Jin, J.-F. Ding, X. Ma, and W.G. Wang

Division of Fuel Cell and Energy Technology, Ningbo Institute of Material Technology and Engineering, Chinese Academy of Sciences, Ningbo, Zhejiang 315201, P.R. China

Solid oxide electrolyzer cells (SOECs) have been considered effective to produce hydrogen at a high conversion efficiency through high temperature electrolysis (HTE) process and has a potential to scale up to a large-scale economy hydrogen source. The crucial issue for the SOEC moving into practical applications is stability. In this paper, investigation was conducted with the focus on the anode degradation using SOEC cells with strontium doped lanthanum manganite (LSM) anode and strontium doped lanthanum ferro-cobaltites (LSCF) anode. The results showed a more stable performance in LSM cells than LSCF cells when testing at 750ºC anode degradation and anode delamination contributed most of performance drop. The LSM cell is thus more suitable for HTE than the LSCF cell due to its better bonding between the electrolyte and anode.

Introduction

Solid oxide electrolyzer cells (SOECs) have been considered effective to produce hydrogen at a high conversion efficiency through high temperature electrolysis (HTE) process (1). Besides its high hydrogen production efficiency, the HTE process using SOECs is simple, clean, and safe, having a potential to scale up to a large-scale economy hydrogen source (2-3). It has thus attracted increasing interests of scientists and researchers in the world in recent years. Moreover, the application of SOEC can be extended to process hydrocarbon fuels by co-electrolysis of CO_2 and H_2O, which makes SOEC more attractive as a new processing method for sustainable fuels (4-5).

Similar to its exact reverse part - solid oxide fuel cell (SOFC), the crucial issue for the SOEC moving into practical applications is stability. Previous investigations showed that the cell in SOEC mode had much higher degradation than the cell in SOFC mode (6-7). Thus investigation on the degradation of SOECs is challenging and important in both theoretical and practical aspects.

The degradation of the SOECs can be categorized into cathode degradation, anode degradation, and electrolyte degradation (7-10). Marina et al. (7) studied a wide range of electrodes of SOFC. They found the Ni/YSZ electrode suffered irreversible degradation under high steam and low hydrogen partial pressures. Laguna-Bercero et al. (10) conducted aging studies on SOEC microtubular cells operated at high voltages and found the cell presented different degrees of damage depending on the analyzed zone. In some regions of the cell, clear degradation of YSZ near to the air electrode side occurred, especially near the oxygen electrode/electrolyte interface. These intergranular defects

propagated through grain boundaries along the electrolyte and progressed towards the hydrogen electrode side. In some cases this effect is accompanied with the delamination of the LSM/YSZ bilayer and even the rupture of the oxygen electrode.

Our previous investigation (11) conducted HTE experiments on the Ni/YSZ cathode-supported solid oxide electrolyzer cells using water steam balanced by 15vol% H2 at a temperature of 750ºC up to 140h. The cells exhibited stable performance while nickel agglomeration was inspected at the hydrogen electrode. Therefore, the effect of hydrogen electrode degradation was limited on the performance of the SOEC. It is thus necessary to investigate the degradation behavior of the air electrode. In this paper, investigation was conducted with the focus on the anode degradation using SOECs with strontium doped lanthanum manganite (LSM) anode and strontium doped lanthanum ferro-cobaltites (LSCF) anode.

Experimental

Experiments were conducted using planar cathode-supported SOECs manufactured at the Division of Fuel Cell and Energy Technology in Ningbo Institute of Material Technology and Engineering (NIMTE), Chinese Academy of Sciences. All cells were Ni-yittria stabilized zirconia (YSZ) cathode supported and had a dimension of 5.8×5 cm^2 with an active area of 16 cm^2. A Ni/YSZ cathode support substrate of 400 μm thick was firstly prepared by tape-casting, then a Ni/YSZ active layer of 10 μm thick and an yttria-stabilized zirconia (YSZ) electrolyte layer of 10 μm thick were sprayed onto the support in turn followed by co-sintering at 1350°C for 3 hours. For cells with LSCF anode, a CGO layer of 5 μm thick was subsequently sprayed on the electrolyte and fired at 1400°C for 4 hours to yield a dense interlayer. The anode functional layer of 20 μm thick was sprayed in a composite form of 50%wt LSCF and 50%wt CGO together with a LSCF cathode collecting layer of 30 μm thick, and sintered in the air at 1050°C for 2 hours. The cells with LSM anode were prepared by spaying a LSM/YSZ cathode functional layer of 25-30 μm thick and a LSM current collector of 30 μm thick over the electrolyte and then sintered at 1080 ºC for 2h.

All the cells were tested in an alumina rig, where gas tubes were sealed with ceramic glass. Platinum and nickel foils were employed as current collecting layers in cathode and anode sides, respectively. Solid LSM slice with channels at anode side provide a well distributed gas flow. Silver mesh was utilized to enwrap the solid LSM slice to decrease the contact resistance between the anode and the current collector. In cathode side, nickel foams were used as gas distribution layer and cushion. Platinum leads were welded on both cathode and anode sides of the cell for voltage testing while the silver bundles were welded to the current collectors on cathode and anode sides for current transport and measurement.

A gas control system including a humidifier, a pump, several flow controller and dew point temperature controller. The schematic illustration of the gas controlling system is shown in Fig. 1. H_2 was used as carrier, and was mixed with steam by means of a heated humidifier. The dewpoint temperature of the steam/hydrogen gas mixture exiting the humidifier was monitored continuously using a dewpoint sensor. The steam/H_2 ratio was then determined by saturated vapor pressure at the dew point temperature. All the HTE

tests were conducted using a steam/H_2 mixture with a mixing ratio of 7 to 3 at the cathode side of the cells while the air was fed in the anode side. Electrochemical performance of the cells with different anodes was tested as a function of time at a constant current density of 0.25 Acm^{-2} at 750ºC.

After testing, the microstructure of the cells was examined by SEM and XRD. The electrochemical impedance spectrum (EIS) were recorded applying an AC voltage with amplitude of 30mV in the frequency range from 2000 kHz to 0.1 Hz at open circuit voltage (OCV) by an IM6ex Electrochemical Workstation (Zahner IM6ex, Germany) during the tests.

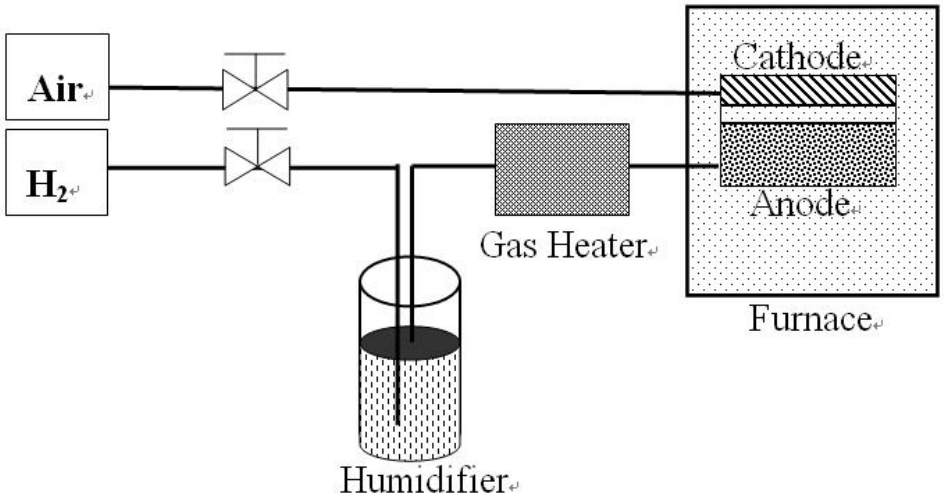

Figure 1. Schematic illustration of gas controlling system.

Results and Discussion

Figure 2 shows microstructures of the electrolyzer cells with LSM and LSCF anode before HTE. It is shown that both the cells before HTE are in good condition: the electrolyte is very dense; both cathode and anode exhibit porous and homogeneous structure; interfaces between electrolyte and cathode, electrolyte and anode are well connected. The thickness of the electrolyte for the LSM cell is ~6 μm and ~10 μm for the LSCF cell. Figure 3 shows the microstructures of the LSM and LSCF cells after HTE for 120 h. No apparent degradation can be observed in the LSM cell, but for the LSCF cell, the cell after HTE exhibited defects between the interface between the cathode/anode and electrolyte. These interface defects were in the form of voids larger than 0.1 μm, and accumulated to form detaching cracks in the interface, especially between the anode and electrolyte. Apparently, the degradation of the cell with LSM anode is much less than the cell with LSCF anode after processing by HTE, and the degradation at the anode side is much more serious than the cathode side.

Figure 4 shows the variation of voltage over time of different cells tested at constant current densities at 750ºC. The two LSCF cells maintained constant voltages for the first

45 h of aging, and then increased electrolysis voltages by 10% during the 45th h to 60th h. After 60th hour, the voltage increase rate slowed down and the cells increased voltage by 6% over 60 h. For the LSM cell, the electrolysis voltage decreased in the first 20 h, and then remained stable for nearly 100 h. The increase of electrolysis voltage at constant electrolysis current indicates the increase in the area specific resistance (ASR) of the cell, and thus degradation of the cell performance. Therefore, the LSM cell had much better performance during THE than the LSCF cell.

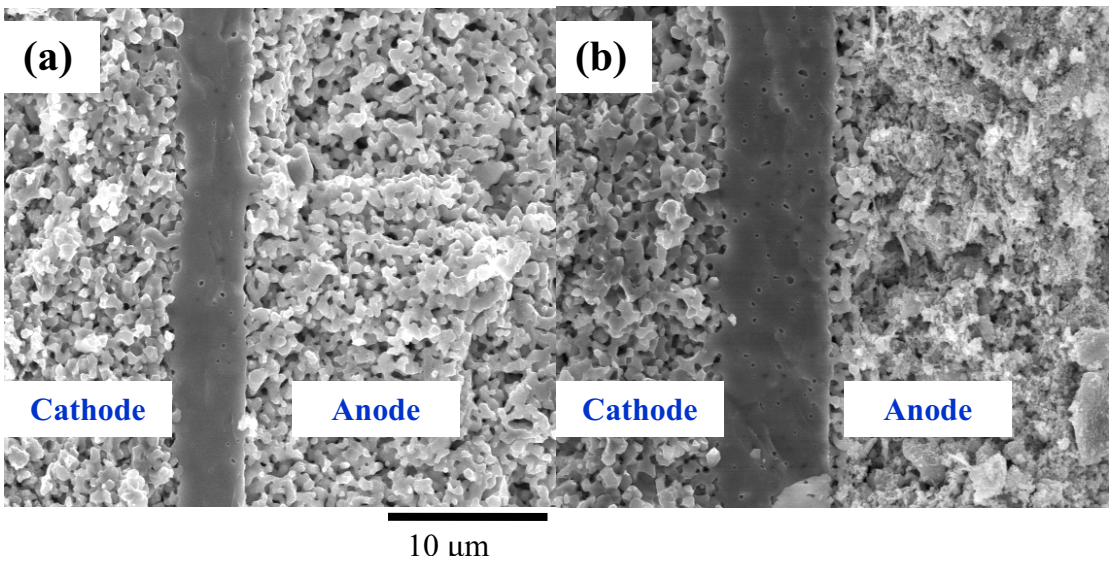

Figure 2. Microstructures before HTE for the cells with (a) LSM anode; (b) LSCF anode.

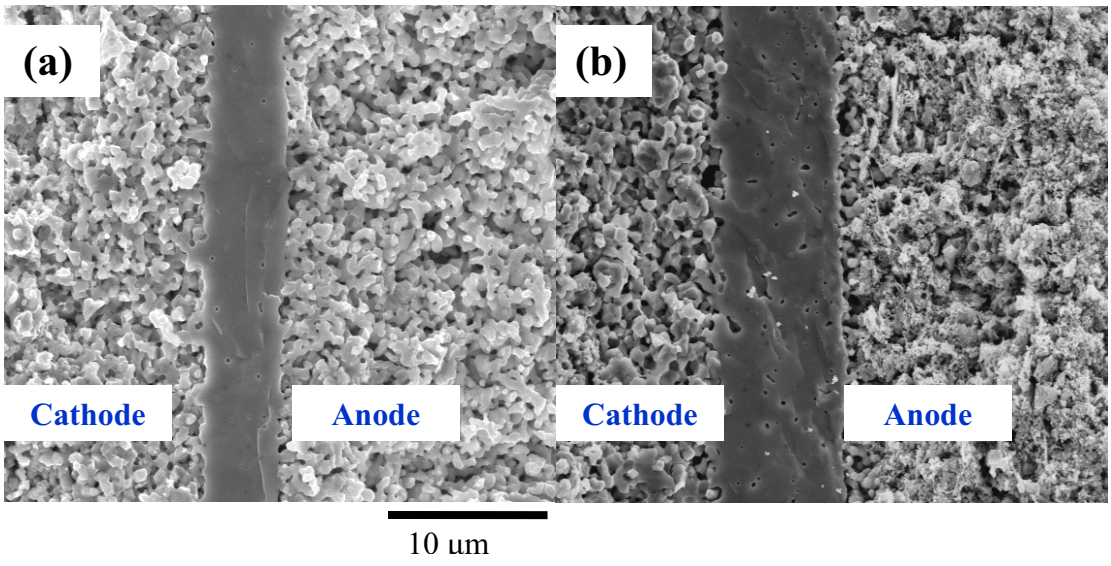

Figure 3. Microstructures after HTE for the cells with (a) LSM anode; (b) LSCF anode.

For cell performance evaluation, the cells before and after HTE were tested and the corresponding V-I curves were recorded and shown in Fig. 5. In the SOFC mode, the cell before and after HTE exhibits similar discharging properties and the cell resistance remains unchanged after over 100 h electrolysis. However, the performances for both cells were not exactly reversible in the SOEC mode after HTE. This irreversibility was

more significant for LSCF cells, which exhibited much higher ASR after HTE in the SOEC mode. For the LSM cell, the change in ASR before and after HTE in the SOEC mode was not significant until the charging current reached 0.5 Wcm^{-2}. Moreover, the ASR for the LSCF cells was apparently larger than the LSM cell after HTE, which may be majorly contributed by ASR increase. This ASR increase may be due to small cracks observed close to the interface between the electrolyte and the anode in the LSCF cells. It is thus concluded that the LSM cell is more suitable for HTE than the LSCF cell due to its better bonding between the electrolyte and anode.

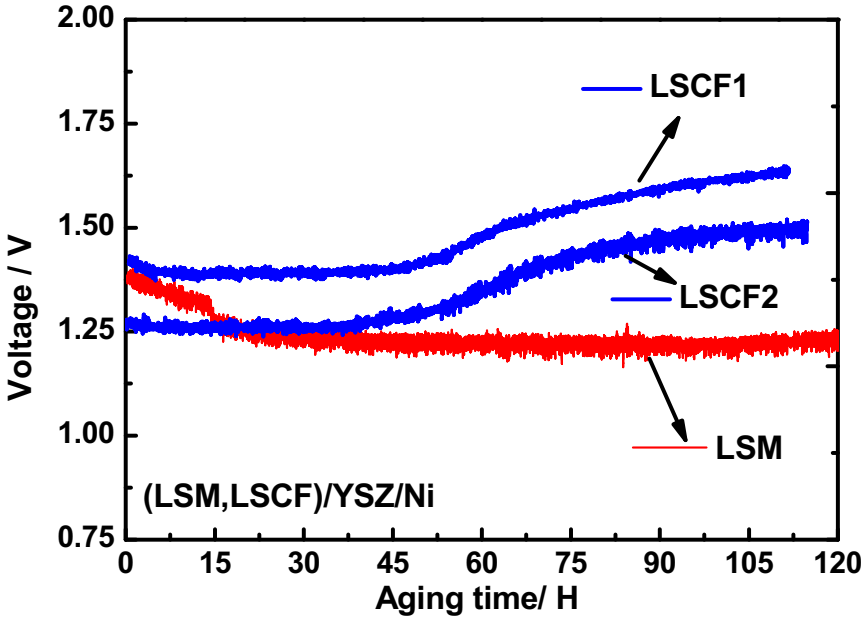

Figure 4. The aging performance of the cells with LSM and LSCF anodes during HTE.

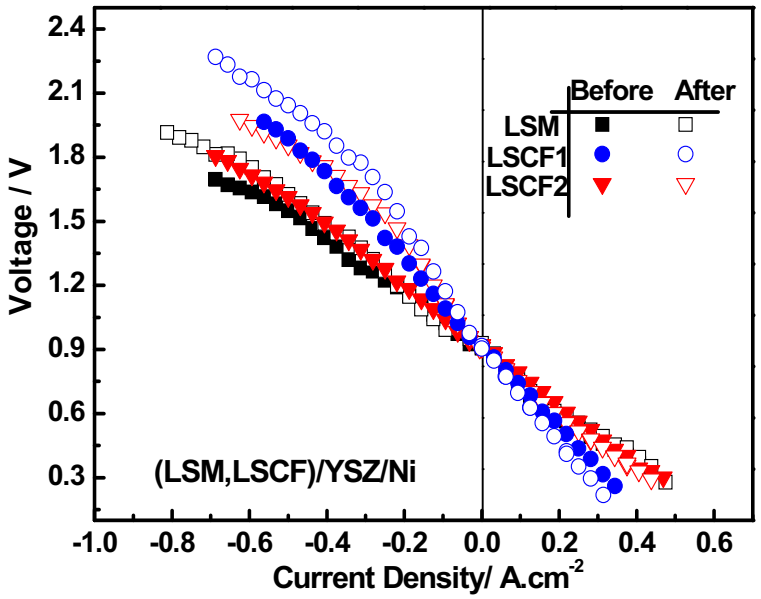

Figure 5. The V-I curves for the cells with LSM and LSCF anodes before and after HTE.

Conclusions

The Ni/YSZ cathode-supported solid oxide electrolyzer cells with LSM and LSCF anode were used for high temperature electrolysis. The cells were tested at a constant current density of 0.25 Wcm^{-2} using water steam balanced by 30vol% H_2 at a temperature of 750ºC up to 120 h. The LSM cell exhibited a more stable and better performance than the LSCF cells when operated in the SOEC mode. The anode degradation and anode delamination contributed most of performance drop. The LSM cell is thus more suitable for HTE than the LSCF cell due to its better bonding between the electrolyte and anode.

Acknowledgments

This work was supported by Chinese Academy of Sciences under Grant No. KJCX2-YW-H21－01.

References

1. A. Brisse, J. Schefold, and M. Zahid, *Int. J. Hydrog. Energy*, **33**, 5375 (2008).
2. J.-W. Kim, A.V. Virkar, K.-Z. Fung, K. Mehta, and S. C. Singhal, *J. Electrochem. Soc.* **146**, 69 (1999).
3. S. C. Singhal, *Solid State Ionics*, **152-153,** 405 (2002).
4. J. Hartvigsen, S. Elangovan, L. Frost, A. Nickens, C. Stoots, J. O' Brein, and J. S. Herring, *Metallurgy* 171 (2008).
5. Z. Zhan, W. Kobsiriphat, J. R. Wilson, M. Pillai, I. Kim, and S. A. Barnett, *Energy Fuels,* **23,** 3089 (2009).
6. A. Hauch, S.H. Jensen, S. Ramousse and M. Mogensen. *J. Electrochem. Soc.*, **153**, A1741 (2006).
7. O. A. Marina, L. R. Pederson, M. C. Williams, G. W. Coffey, K. D. Meinhardt, C. D. Nguyen, and E. C. Thomsen, *J. Electrochem. Soc*. **154,** B452 (2007).
8. M. A. Laguna-Bercero, S. J. Skinner, and J. A. Kilner, *J. Power Sources,* **192**, 126 (2009).
9. A. V. Virkar, *Int. J. Hydrog. Energy*, **35**, 9527 (2010)
10. M. A. Laguna-Bercero, R. Campana, A. Larrea, J. A. Kilner, and V. M. Orera, *J. Power Sources,* **196**, 8942 (2011).
11. C. Xu, J. F. Ding, T. S. Li and W. G. Wang, in *Proceedings of 9th European Solid Oxide Fuel Cell Forum*, P. Connor Editor, PV 14, p. 14-72, European Fuel Cell Forum Proceeding series, Luthern, Switzerland (2009).